2010 IEEE International Conference on Robotics and Automation
Anchorage Convention District
May 3-8, 2010, Anchorage, Alaska, USA

Peristaltic locomotion with antagonistic actuators in soft robotics

Sangok Seok, Cagdas D. Onal, Robert Wood, Daniela Rus, and Sangbae Kim

***Abstract*— This paper presents a soft robotic platform that exhibits peristaltic locomotion. The design principle is based on the unique antagonistic arrangement of radial/circular and longitudinal muscle groups of Oligochaeta. Sequential antagonistic motion is achieved in a flexible braided mesh-tube structure with NiTi coil actuators. A numerical model for the mesh structure describes how peristaltic motion induces robust locomotion and details the deformation by the contraction of NiTi actuators. Several peristaltic locomotion modes are modeled, tested, and compared on the basis of locomotion speed. The entire mechanical structure is made of flexible mesh materials and can withstand significant external impacts during locomotion. This approach can enable a completely soft robotic platform by employing a flexible control unit and energy sources.**

I. Introduction

Peristalsis is common in small limbless invertebrates such as Oligochaeta (worms). Oligochaeta need to deform their body to create the essential processes of locomotion (engagement, propulsion, and detachment) in contrast to legged locomotion which involves legs for the same functions. By deforming their body, worms can modulate friction forces of ground contact points at the body. For applications that require operation in limited space, peristalsis can enable robust locomotion without the need for complicated limb structures.

Several worm-like platforms have been developed for operation in confined spaces, such as with endoscopy. Serial configurations of pneumatic actuators generated peristaltic locomotion for an endoscope that maneuvers inside a small tube [4]. Alternatively, moving magnetic fields can drive sequential expansion of each segment when filled with a magnetic fluid [8]. Piezoelectric actuators have demonstrated reciprocal motion of two halves of the platform with directional skin [2]. Finally, NiTi actuators have been used to contract each elastic segment and then extend by releasing the stored elastic energy in the structure [5].

This paper presents peristaltic locomotion using the unique characteristics of a mesh-tube driven by antagonistic circular and longitudinal NiTi muscle groups. The body structure consists of an elastic fiber mesh tube, which enables the antagonistic arrangement between radial/circular muscle and longitudinal muscle [3]. The kinematic model of mesh tube deformation describes how peristaltic contraction enables locomotion of the platform. To ensure a minimum number of actuators, induced antagonistic actuation is introduced and experimentally validated. Multiple gait modes are chosen and tested on the prototype and analyzed to determine locomotion speed and efficiency.

Sangok Seok, Cagdas D. Onal, Sangbae Kim, and Daniela Rus are, respectively, a graduate student, a post doctoral fellow, and faculty members in Massachusetts Institute of Technology, Cambridge, MA 02139, USA sangok@mit.edu

Robert Wood is a faculty member in School of Engineering and Applied Sciences at Harvard University, Cambridge, MA 02138, USA

This work is supported in part by Defense Advanced Research Projects Agency (DARPA) grant W911NF-08-C-0060 (Chemical Robots)

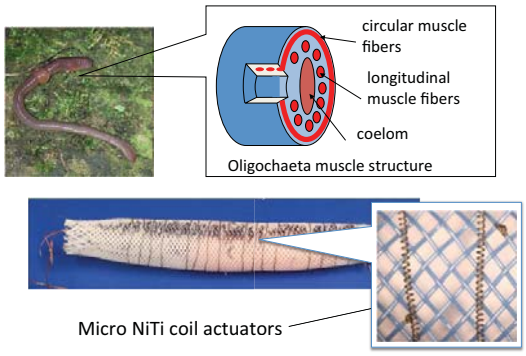

Fig. 1. Oligochaeta utilize antagonistic radial and longitudinal deformation of the body. The meshworm prototype exhibits peristaltic locomotion induced by a similar antagonistic configuration.

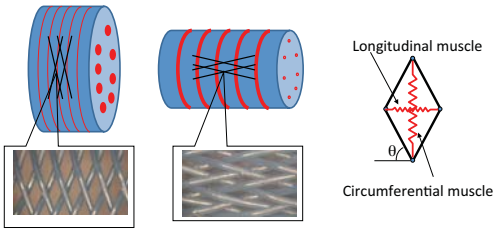

Fig. 2. The mesh structure can transmit power from the longitudinal direction to the radial direction and vice versa.

II. Antagonistic Actuation in Soft Bodies

Natural muscles generate power in contraction. Vertebrates attain flexion and extension motions from intricate kinematics of rigid bones, joints with cartilage, and contracting muscles in antagonistic arrangements. In invertebrates, a hydrostatic skeleton enables shape change and stiffness modulation. Oligochaeta, in particular, employ an antagonistic pairing of radial muscles and longitudinal muscles. Figure 1 shows the arrangement of muscle groups found in Oligochaeta.

Antagonistic circular or radial muscles and longitudinal muscles control movements of the hydrostatic bodies of earthworms [6]. Coelom in each septum contains liquid that works as fluidic transmission between the longitudinal and radial directions. With this divided cavity filled with fluid,

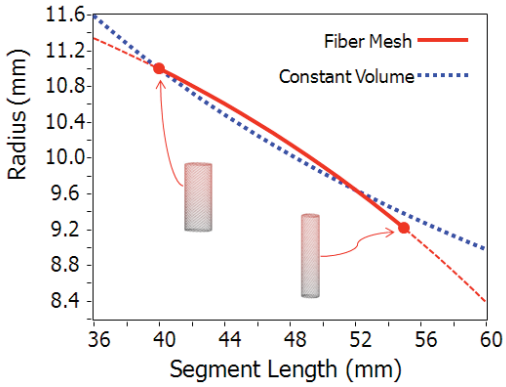

Fig. 3. Comparison between hydrostatic cylindrical deformation found in nature and deformation in fiber mesh-tube.

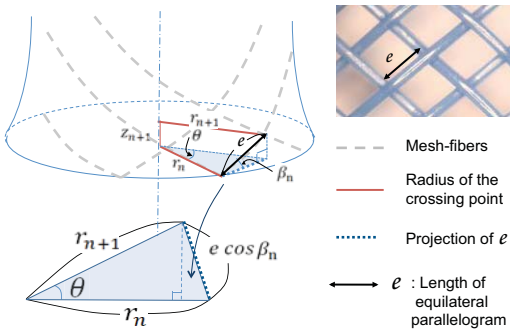

Fig. 4. The projection of an individual fiber in the mesh structure to the plane perpendicular to the axis of the mesh-tube. The length of a spiral strand does not change over antagonistic deformation but changes radius and height.

each segment of the worm can deform with a constant volume constraint [1], [6]. The hydrostatic skeleton can be thought of as an elastic cylindrical container that varies radius and length subject to fixed internal volume.

With mesh tubes, a similar antagonistic configuration has been previously demonstrated [3]. The mesh tube structure is composed of multiple spiral polymeric fibers woven into a tube shape. An increase in the pitch of the individual spiral fiber results in a reduction of its radius and decrease in pitch expands the radial dimension of the spiral. Figure 3 shows the relationship between length and radius in earthworms (constant volume) and in the mesh-tube. In a constant volume cylinder, the relationship between radius and length of the cylinder follows (1). In a mesh-tube structure, the relationship between radius and length follows (2).

$$r^2 l = Constant \tag{1}$$

$$Ar^2 + l^2 = Constant \tag{2}$$

where r is radius and l is length of the cylinder and where A is characteristic coefficient of the cylinder. Correspondingly, parabolic and circular curves are found in Figure 3.

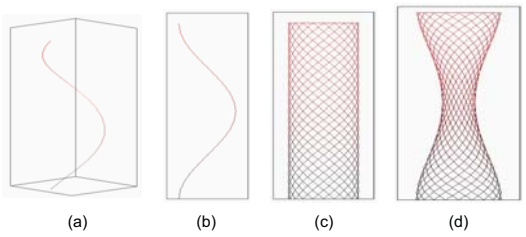

Fig. 5. (a) One spiral strand shown in 3D space. Mesh-tube is woven from multiple strands of these polymeric spirals. (b) Projection of an individual spiral to any plane which contains the worm's longitudinal axis is a sinusoid. (c) Recreation of the mesh-tube on a 2D surface is a combination of sinusoidal curves. (d) Simulated deformation.

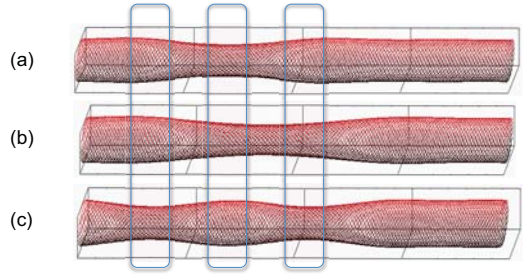

Fig. 6. Simulation results show three different actuation mode. (a)The 2nd actuator is actuated. (b)The 2nd and the 3rd actuators are actuated. (c)The 1st and the 3rd actuator are actuated.

III. Peristaltic Locomotion

A. Simulation

The mesh-tube structure consists of multiple spirals. Each spiral is kinematically identical to a stretched spring. Under stress, the tube deforms in a antagonistic regime with a constraint given in (2). The basic element is an rhombus. Mathematically, we can assume the mesh-tube is composed of a number of rhombi, shown in figure 4 using a cylindrical coordinate. The lengths of each side are assumed to be equal and remain constant under deformation. Also, each rhombus can bend out of plane along the diagonal line perpendicular to the longitudinal axis of the tube. In other words, each rhombus can create two equilateral triangles and the two triangles can bend within a limited angle. In figure 4, e remains constant and the radii of mesh crossing points changes depending on the deformation. Also, θ in this case remains constant since the number of mesh crossing points along the perimeter remains constant.

$$r_{n+1}^2(sin\theta)^2 + (r_n - r_{n+1}(cos\theta)^2 = e^2(cos\beta_n)^2 \tag{3}$$

$$\beta = cos^{-1}\left(\frac{\sqrt{r_{n+1}^2 + r_n^2 - 2r_{n+1}r_n cos\theta}}{e}\right) \tag{4}$$

$$z_{n+1} = esin\beta_n \tag{5}$$

Through (3) (5), we can calculate z_{n+1} as a function of r_n. Once the radius profile as a function of z of the tube is known, we can obtain geometrical configuration of the entire mesh structure. The radius profile is experimentally verified

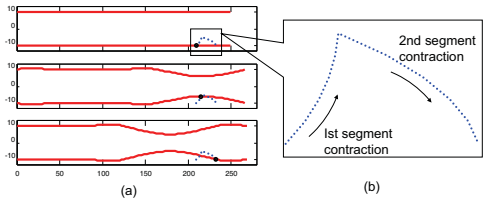

Fig. 7. The red solid lines represent mesh-tube deformation in the sagittal plane (left). Magnification of the trajectory of the black point (right). The black point travels through the air during the contraction wave passes.

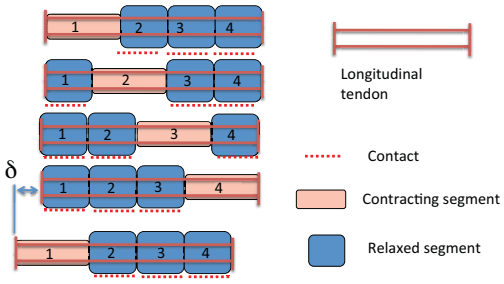

Fig. 8. An example of peristaltic locomotion sequence by induced antagonism in the sagittal plane. Dotted red line represent contact with the ground. Longitudinal tendons keep the body length constant. Contraction of radial actuators induces radial expansion of adjacent segments.

since the stress-strain analysis of the weave of the elastic strands becomes excessively complicated.

The motion of the system was simulated using a numerical model for the mesh-tube structure. Figure 6 shows the simulated deformation of the mesh-tube. Sequential radial contractions of the segments result in peristalsis. Figure 7 shows how sequential contraction of segments can induce robust locomotion. The red solid lines represent body deformation in several time sequences between first and second contractions. The dotted blue line represents the trajectory of a point of the skin contacting the ground periodically when segments contract radially and expand axially. Assuming that the ground is flat, the contact point releases from the ground with radial contractions and travels through a swing phase forward of the initial contact point. If trajectories of a number of points along the tube are considered, they create a traveling wave. This resembles leg trajectories found in small arthropods, which create a couple of waves of trajectories of legs instead of body deformation. The trajectory depends on the relative position relative to the segment border. However, if the segments are small enough to create a pseudo-continuous wave in the body deformation, every point will detach from the ground, progress, and land on the ground. This simulation shows how a peristaltic wave created by antagonistic radial and longitudinal actuators can create effective locomotive without legs.

B. Induced antagonism

Two different arrangements of NiTi actuators were considered for the mesh-tube prototype. The first arrangement

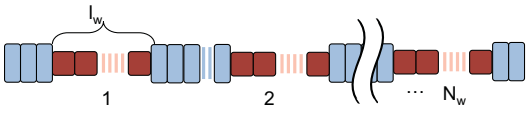

Fig. 9. A general expression of all possible gaits. N_w represents the number of gaits and l_w represents the number of contracted segments (length of wave)

consists of a series of individual active antagonistic segments with both longitudinal and radial actuators. In this case, each segment can independently contract in radial or longitudinal directions. This enables independent control for various gaits but introduces high complexities in fabrication and in synchronizing multiple NiTi actuators in order to create effective gaits. In particular, NiTi is sensitive to heat dissipation and thus it becomes challenging to synchronize multiple actuators in phase. The second method utilizes induced antagonistic actuators. Instead of adding longitudinal actuators at each segment, flexible but inextensible tendons are attached through the body along the longitudinal direction. The longitudinal tendon keeps the body length constant, thus any local longitudinal expansion creates other sections' longitudinal contraction. The constant length constraint forces neighboring segments to contract longitudinally and expand radially, hence the antagonism. Figure 8 shows how the length constraint enables coupled behavior among segments. Consider the bottom sequence in Figure 8. The radial actuators in the first segment contract radially and expand in the longitudinal direction. This also induces reduction of last segment's length because of the total length restriction by the tendons. This method enables induced antagonism between deformation in longitudinal and radial direction without a passive spring return, which causes a significant bandwidth limitation. A prototype using the second method is described in section IV. Quillin expresses the speed of the worms by protrusion times and stance time [7] with stride length. His analysis includes the total length change in worms. Assuming the total number of body segments is large enough, which is consistent with worms' case, a general expression for all the gaits available using this approach is shown in Figure 9 Thus, the theoretical speed of the locomotion is,

$$Speed = \delta \times N_w \times l_w \times f \tag{6}$$

where δ is the length change of each segment, N_w is number of waves of contraction, l_w is a number of segments contracted in single wave, and f is the frequency of the waves.

IV. Experimental Results

A. Controller

A key goal of the experiments has been to test and measure the effectiveness of several locomotion gaits for the Meshworm. We developed a gait controller using LabVIEW software and NI Single-Board RIO (NI sbRIO-9642). Figure

10 shows a screenshot of the control panel. This experimental setup allows various actuation sequences, the number of active segments and duration.

For a standalone implementation of the Meshworm, we used a custom PCB as an embedded controller. Figure 11 shows the control board which has a very small form-factor that easily fit inside the robot body. Equipped with an ATmega88PA microcontroller, the PCB has eight digital outputs that are used to drive eight MOSFETs, which are connected to a separate power line to protect the microcontroller from large currents. Actuation power is supplied by an on-board step-up regulator. Using the digital outputs, we can regulate power to the individual NiTi coils to produce different gaits. In addition, the board has eight 10 bit A/D channels for closed-loop implementation.

We built an experimental prototype using a polyester braided mesh tube. The tube is approximately 22mm in diameter and each strand is 0.25mm in diameter. The length of the tube is approximately 20cm in the unloaded state. The unloaded state is created by annealing the polyester mesh-tube held with a metal pipe with the desired diameter. The annealing temperature is approximately 125°C and the duration is 10 min. Since polyester is a thermoplastic, the unloaded state can be reconfigurable with different sizes of the metal pipe. NiTi coil actuators introduced in [3] are used. The wire diameter is 100 μm and the coil diameter is 400 μm. Five NiTi actuators are wrapped around the tube.

NiTi actuation is based upon a solid-state phase transition controlled by temperature changes. Since this is a thermal process, these actuators are typically rather inefficient. Greater efficiency can be achieved by rapid current pulses as opposed to constant currents. Figure 12 compares radius changes with various current settings. Using a segment of the mesh-tube and a circumferential actuator, the radius profile is plotted as a function of time. If the 400mA current with shorter pulse time is compared with 200mA current setting, it is clear that higher current with a shorter pulse duration results in quicker and more energy efficient actuation. This high current value, however, yields a steady-state temperature above the glass transition temperature of the body material

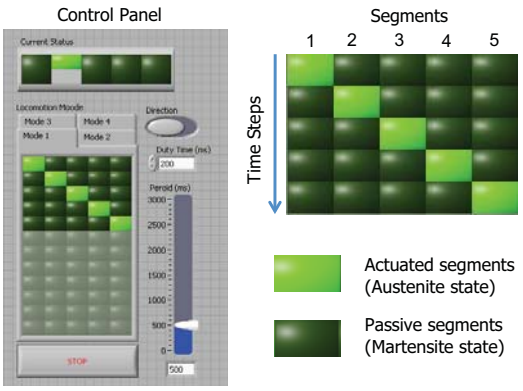

Fig. 10. Control panel used for generating various gait for the meshworm prototype.

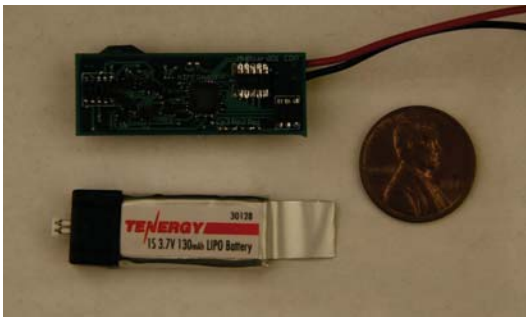

Fig. 11. A micro-controller prototype for gait generation and a Li-Poly battery.

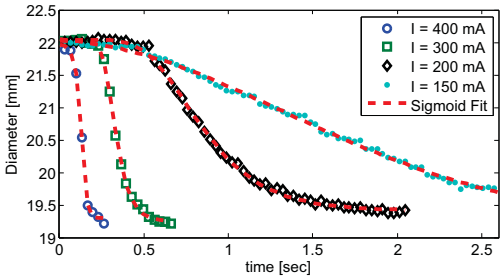

Fig. 12. Radius of the mesh as a function of time in different current settings on circumferential actuators.

and hence should be applied for short time intervals only. The given pulse consumes about 3.2 J of energy.

Additional experiments include measurements of the length change of each segment, displacement of the mesh-tube, and overall locomotion speed. An external camera system (Microsoft LifeCam VX-3000) is used for capturing motions of the prototype and the prototype has motion tracking markers at the borders between the segments. As the mesh-tube moves, the camera tracks the distance between the markers and the head position of the tube for the overall travel. The frame rate is 15 fps with 640 x480 resolution for locomotion tests and 30 fps with 320x240 for contraction experiments. The current applied to the actuators is 400mA with 200ms duration.

We tested two different modes (gaits). The first mode is the short-wave mode: $N_w = 1$, $l_w = 1$. The second mode is the long-wave mode where two adjacent segments are

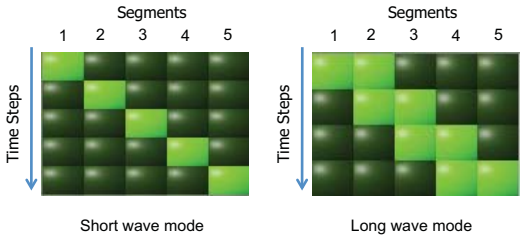

Fig. 13. Two different gaits were tested: short wave mode has one segment contracted at a time. Long wave mode have two segments contracted at a time.

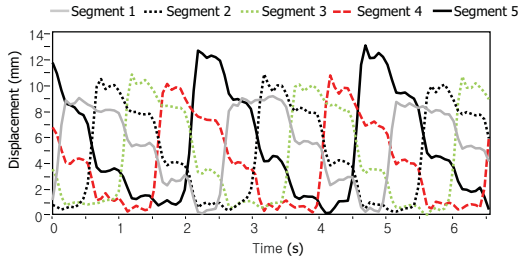

Fig. 14. Lengths of segments as a function of time. The data is filtered at 5 Hz.

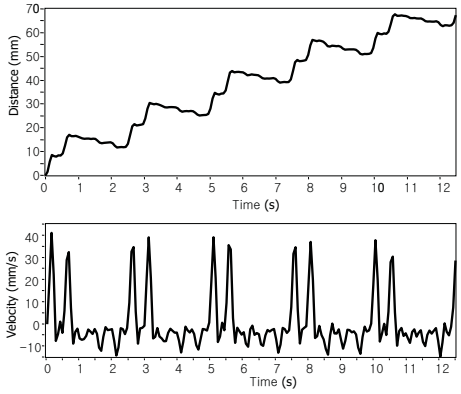

Fig. 15. Displacement (top) and velocity (bottom) of the prototype using the short wave mode. The data is filtered at 5 Hz.

contracted at a time: $N_w = 1$, $l_w = 2$. We figure that the distance between two waves in multi-wave mode should be long enough because it needs cooling time. Therefore, the implementation of gaits with more than one waves for Meshworm which has only five segments results in inefficient locomotion.

B. Closed-loop Control

The NiTi coil actuators are sensitive to environment conditions (*e.g.* ambient temperature, air flow). This makes open-loop control ineffective and inconsistent. For reliable actuation of NiTi, a feedback control is implemented using small hall-effect sensor/magnet pairs that measure the radius of a segment of the body. The desired radius can be achieved by controlling the time interval of current through the NiTi coils based on the signal from magnet sensor.

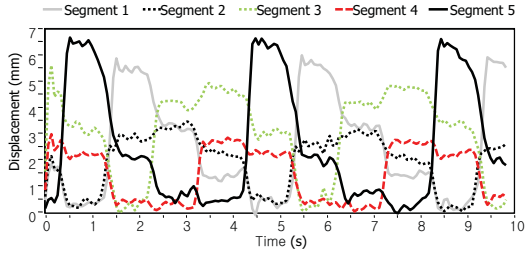

Fig. 16. Using the long wave mode, five segments' lengths are plotted as a function of time. The data is filtered at 5 Hz.

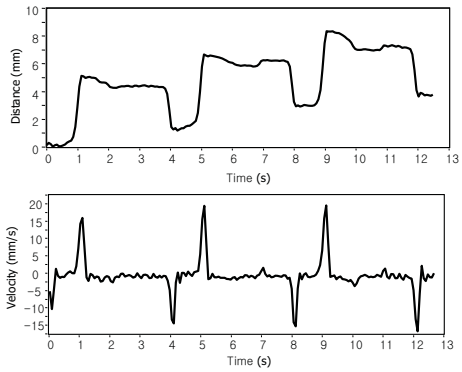

Fig. 17. Displacement (top) and velocity (bottom) of the prototype using the long wave mode. The data is filtered at 5 Hz.

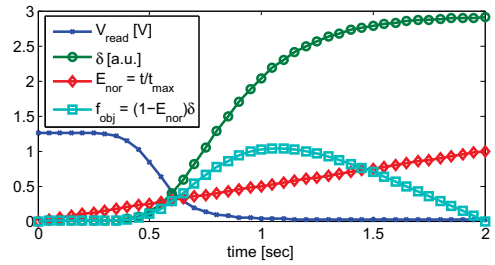

Fig. 18. Functions used to achieve the objective function. Voltage from the hall-effect sensors are converted to deflection data by $\delta = V^{-1/3} - \delta_0$. Energy consumption is normalized by a maximum time interval t_{max} = 2 sec.

From Figure 12, we experimentally determined that the deflection (δ) of a single segment can be described by a general sigmoid function and energy consumption is directly proportional to time ($E = I^2Rt$). Normalizing the energy with the energy consumed at the maximum duration (I^2Rt_{max}) yields $E_{nor} = t/t_{max}$. The voltage reading from the hall-effect sensor has approximately an inverse cubic relation with the deflection of the radius. This relation gives $\delta = V^{-1/3} - \delta_0$ in arbitrary units, where δ_0 describes the initial separation between the sensor and the magnet. Borrowing ideas of optimization theory, we chose a steepest descent algorithm on an objective function $f_{obj} = (1 - E_{nor})\delta$, which corresponds to a metric that defines the trade-off between power consumption and deflection as seen in Fig. 18. Using this method, an optimal current interval was experimentally found as shown in Fig. 19.

V. Discussion

Figure 14 shows a plot of segment lengths as a function of time. From this result, we can calculate theoretical speed due to (6). δ average is 9.98 mm, f = 1/2.5 Hz, and $N_w = I_w = 1$, so theoretical speed becomes 3.99 mm/s. Also, actual speed can be found from displacement plot in Figure 15. It is 3.47 mm/s which is 13% lower than theoretical speed.

Unlike the ideal condition shown in Figure 8, the length change does not complete at one step since a finite time(2 seconds) is required for NiTi to shift its state from austenite

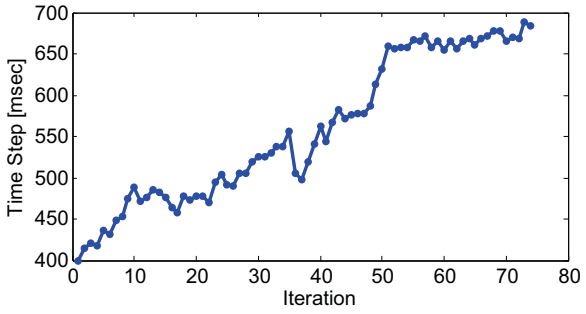

Fig. 19. Experimental results using a steepest descent algorithm on f_{obj}. Time steps gradually converge to an optimal value of $\tau \approx 680$ msec based on this metric.

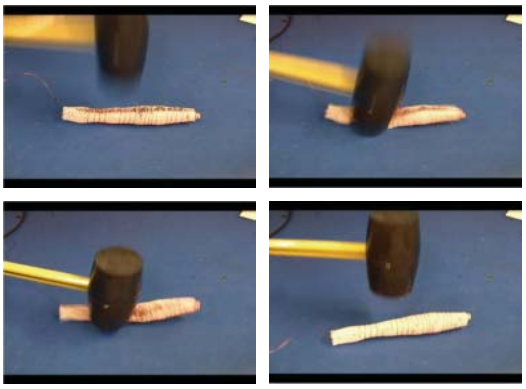

Fig. 20. An experiment to verify the robustness of the mesh-tube platform is performed. During locomotion, a rubber hammer impacts the mesh tube and the mesh tube experiences substantial amount of impact on the body. The results show that the mesh tube can continue locomotion after several impacts from the hammer.

to martensite. When a radial actuator contracts, the corresponding segment elongates in the longitudinal direction. When the next segment contracts, it elongates and shortens the previously elongated segment where the radial actuator becomes martensite and ready to detwine. The segment's length does not become original length shown as the minimum value in Figure 14. This imperfection causes backward motion of the body in Figure 15. The long wave mode is not as efficient as the short wave mode in practice. Theoretically, the speed should be proportional to length of the wave. Since the total length of the prototype has only five segments, there are only three unactuated segments. The mesh-tube could not hold the position very well with only three segments grounded.

Variations in the change of length is caused by errors in the manufacturing process. The short-wave mode is the most reliable mode among gaits we have tried. When actuation shifts from one segment to adjacent one, three radially-expanded segments remain still holding the ground with friction forces. As discussed in the *peristaltic locomotion* section, the trajectory of points lift from the ground as the wave passes. However, in practice, the real trajectory tends to slide along the ground surface with several possible reasons such as imperfections in manufacturing, variation in actuator strength, and lack of friction between the body and the ground.

VI. CONCLUSIONS AND FUTURE WORKS

Peristaltic locomotion by a soft bodied robot with antagonistic actuation is successfully accomplished in this study. Speed and energy efficiency can be optimized by further investigation of gait generation and actuator fabrication. Additionally, more functions can be added by increasing in number of degrees of freedom. The mesh-tube prototype has five segments whereas biological counterparts have close to 100 of segments. The length of the each segments in the mesh-tube is relatively longer compared to that of an earthworm. This prevents smooth wave travel through the body and implementation of various gaits and functions. The current manufacturing process involves hand construction and connections of the NiTi actuators to the mesh structure. For versatile performance of the platform, advances in the fabrication methods will enable a greater number of segments in a given length, and hence smoother waves and more efficient gaits. Direction changes introduced in [3] can be applied to the mesh-tube platform to increase maneuverability. Since the platform contains no rigid components that may fail by external impacts, this approach can open a new space of applications for robust morphable robots. With further development of a microprocessor and battery with flexible form factors, this approach suggests a new paradigm of completely soft robotic systems, that can demonstrate significant body morphing and versatile locomotion capabilities.

REFERENCES

[1] G. Chapman. Of the movement of worms. *Journal of Experimental Biology*, 27:29–39, 1950.

[2] B. Kim, S. Park, C. Jee, and S. Yoon. An earthworm-like locomotive mechanism for capsule endoscopes. In *Proceedings - IEEE International Conference on Intelligent Robots and Systems*, pages 2997– 3002, 2005.

[3] S. Kim, E. Hawkes, K.J. Cho, M. Jolda, J. Foley, and R.J. Wood. Micro artificial muscle fiber using niti spring for soft robotics. In *Proceedings - IEEE International Conference on Intelligent Robots and Systems, 2009(accepted)*.

[4] E.V. Mangan, D.A. Kingsley, R.D. Quinn, and H.J. Chiel. Development of a peristaltic endoscope. In *Proceedings - IEEE International Conference on Robotics and Automation*, volume 1, pages 347–352 vol.1, 2002.

[5] A. Menciassi, S. Gorini, G. Pernorio, and P. Dario. A sma actuated artificial earthworm. In *Proceedings - IEEE International Conference on Robotics and Automation*, volume 4, pages 3282–3287, 2004.

[6] G. E. Newell. The role of the coelomic fluid in the movements of earthworms. *Journal of Experimental Biology*, 27:110–122, 1950.

[7] K. J. Quillin. Kinematic scaling of locomotion by hydrostatic animals: ontogeny of peristaltic crawling by the earthworm lumbricus terrestris. *Journal of Experimental Biology*, 202:661–674, 1999.

[8] N. Saga and T. Nakamura. Development of a peristaltic crawling robot using magnetic fluid on the basis of the locomotion mechanism of the earthworm. *Smart Materials and Structures*, 13(3):566–569, 2004.